Theoretical study on Electrocatalytic Reduction of CO_2 over Co based nitrogen doped graphene nanolayer supported diatomic catalyst

Ke Li, Bingjie Ye, Wei Li*, Shixi Liu*

School of Chemical Science and Engineering, National Demonstration Center for Experimental Chemistry and Chemical Engineering Education, Yunnan University, Chenggong Campus, Yunnan University, South Section, East Outer Ring Road, Chenggong District, Kunming, Yunnan province, People's Republic of China.

Table. S1. The single-point energy of CoN_3-CoN_3@NGr-a, *CO_2 (CoN_3-CoN_3@NGr-a), and the difference between these two.

	CoCoa	*CO_2 (CoCoa)	Difference
DZP/TZP-Small	-628.80	-651.84	-23.04
DZP/TZP-None	-630.12	-653.43	-23.30
DZP/TZP-Large	-628.28	-651.47	-23.20
DZ-Small	-603.82	-624.48	-20.67
TZ2P-Small	-640.14	-664.29	-24.14
QZ4P-Small	-641.77	-665.65	-23.87

Table. S2. The formation energy (E_f) of NGr, and the adsorption energy of NGr (AE_1) with CO_2.

	NGr-a	NGr-s
E_f (eV)	5.88	8.26
AE_1 (eV)	-0.42	0.01

Table. S3. Bader analysis values ($|e^-|$) of Co, M^2 and CO_2 on M^1N_3-M^2N_3@NGr before (Co-1, M^2-1) and after CO_2 adsorption (CO_2, Co-2, M^2-2). Adsorption energy (AE_2) of transition metal atoms loaded on NGr by M^1 and M^2.

Catalyst	Co-1	M^2-1	CO_2	Co-2	M^2-2	AE_2
CoCoa	0.69	0.69	-0.54	0.84	0.89	-13.09
CoCra	0.61	1.14	-0.64	0.76	1.41	-12.83
CoCua	0.70	0.67	-0.68	0.78	0.76	-12.36
CoFea	0.65	0.89	-0.50	0.88	0.91	-13.85
CoMna	0.60	1.07	-0.57	0.77	1.24	-12.52
CoNia	0.73	0.58	-0.38	0.90	0.63	-14.05
CoCos	0.86	0.86	-0.41	0.90	0.97	-11.44
CoCrs	0.89	1.20	-0.65	0.93	1.43	-10.64
CoCus	0.88	0.68	-0.33	0.90	0.84	-9.20
CoFes	0.88	1.04	-0.50	0.90	1.17	-11.54
CoMns	0.89	1.10	-0.62	0.91	1.30	-10.73
CoNis	0.87	0.80	-0.47	0.90	0.87	-10.73

Table. S4. The Gibbs free energy change (ΔG (eV)) of CO_2RR reaction intermediates on the active site of M^1N_3-M^2N_3@NGr-a (M^1=Co and M^2=Co, Cr, Mn, Ni) surface.

	CoCoa	CoCra	CoMna	CoNia
*H	-0.02	0.36	0.26	0.59
*COOH	-0.03	0.03	-0.11	0.46
*OCHO	0.13	0.29	0.38	0.99
*OCHOH	0.52	0.94	0.81	0.58
*CO	-1.43	-0.51	-0.31	-0.73
*CHO	2.10	0.49	0.01	0.19
*CO*CO	-0.37	-1.09	-1.17	0.02
*CHO*CO	0.25	0.57	0.41	0.26
*COH*CO	1.31	1.02	0.97	1.28
*OCHCO	0.82	0.17	0.35	-0.46
*CHOH*CO	0.84	0.36	0.86	1.06

*OCHCOH	0.29	0.02	0.06	0.37
*OCH_2COH	0.33	-0.17	-0.14	0.68
*OCH_2CHOH	-0.78	-0.29	-0.43	-0.59
*OCH_2CH	0.39	-0.19	0.29	0.55
*OCH_2CH_2	-1.10	-0.93	-0.53	-0.56
*O+C_2H_4	-0.85	-0.32	-1.03	-1.15
*OCH_2CH_3	-1.45	-0.65	-0.23	-1.93
CH_3CH_2OH	0.30	0.83	-	-0.41
*OH	-	-	-0.01	-
*H2O	-	-	0.24	-
H2O	-	-	-0.15	-

Table. S5. The Gibbs free energy change (ΔG (eV)) of CO_2RR reaction intermediates on the active site of M^1N_3-M^2N_3@NGr-a (with M^1=Co and M^2=Cu, Fe) surface.

	CoCua		CoFea
*H	1.01	*H	0.18
*COOH	0.14	*COOH	0.03
*OOCH	0.20	*OOCH	0.15
*OCHOH	0.25	*OCHOH	0.33
*CO	-0.55	*CO	-1.12
*CHO	0.22	*CHO	0.88
*CO*CO	0.01	*CO*CO	-0.82
*CHO*CO	0.27	*CHO*CO	0.60
*COH*CO	1.89	*COH*CO	-0.85
*OCHCO	0.91	*COH*CHO	2.22
*CHOH*CO	0.61	*C*CO	-0.71
*CHOHCO	-0.85	*CCO	-0.81
*CHOHCOH	0.53	*CCOH	0.78
*CHCOH	-0.24	*CCHO	-0.15
*CH_2COH	-1.44	*CCHOH	-0.29
*CH_2CHOH	-0.47	*CCH	0.06
*C_2H_3	-0.37	*CCH_2	0.36
*C_2H_4	-0.72	*C_2H_3	-1.73
C_2H_4	0.50	C_2H_4	0.01
*C_2H_5	-0.32	-	-
C_2H_6	-1.11	-	-

Table. S6. The adsorption energy (AE_3) of OC_2H_4 on M^1N_3-M^2N_3@NGr-a (M^1=Co and M^2=Co, Cr, Mn, Ni).

	CoCoa	CoCra	CoMna	CoNia
AE_3 (eV)	-4.32	-5.81	-8.12	-2.74

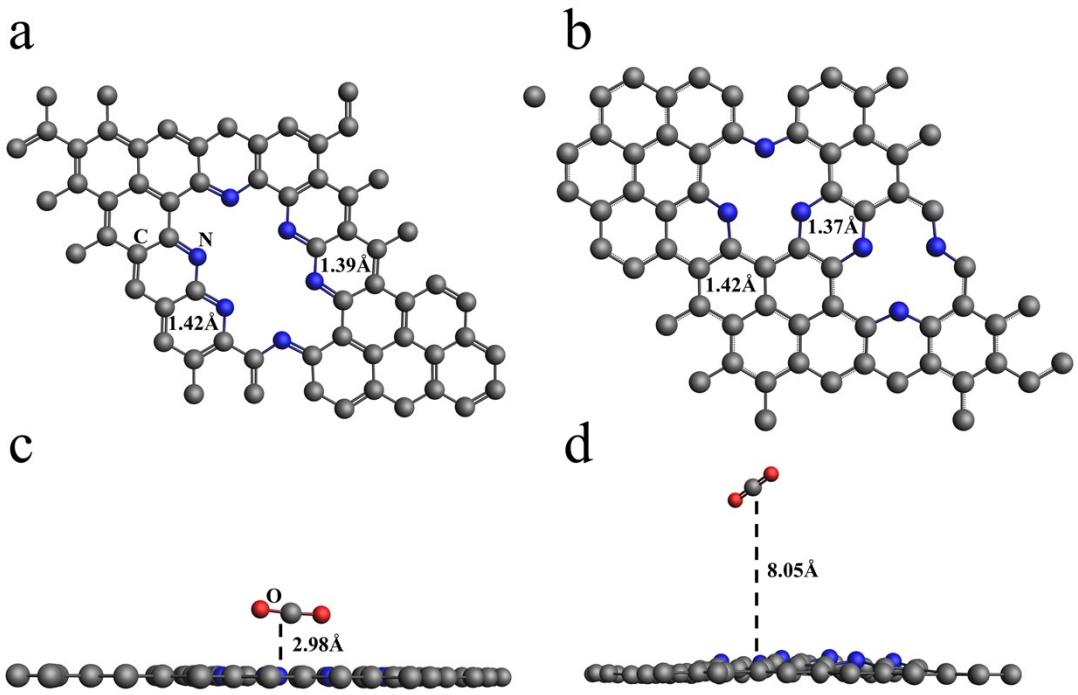

Fig. S1. The structural model of NGr-a (a), NGr-s (b), NGr-a adsorbing CO_2 (c), NGr-s adsorbing CO_2 (d).

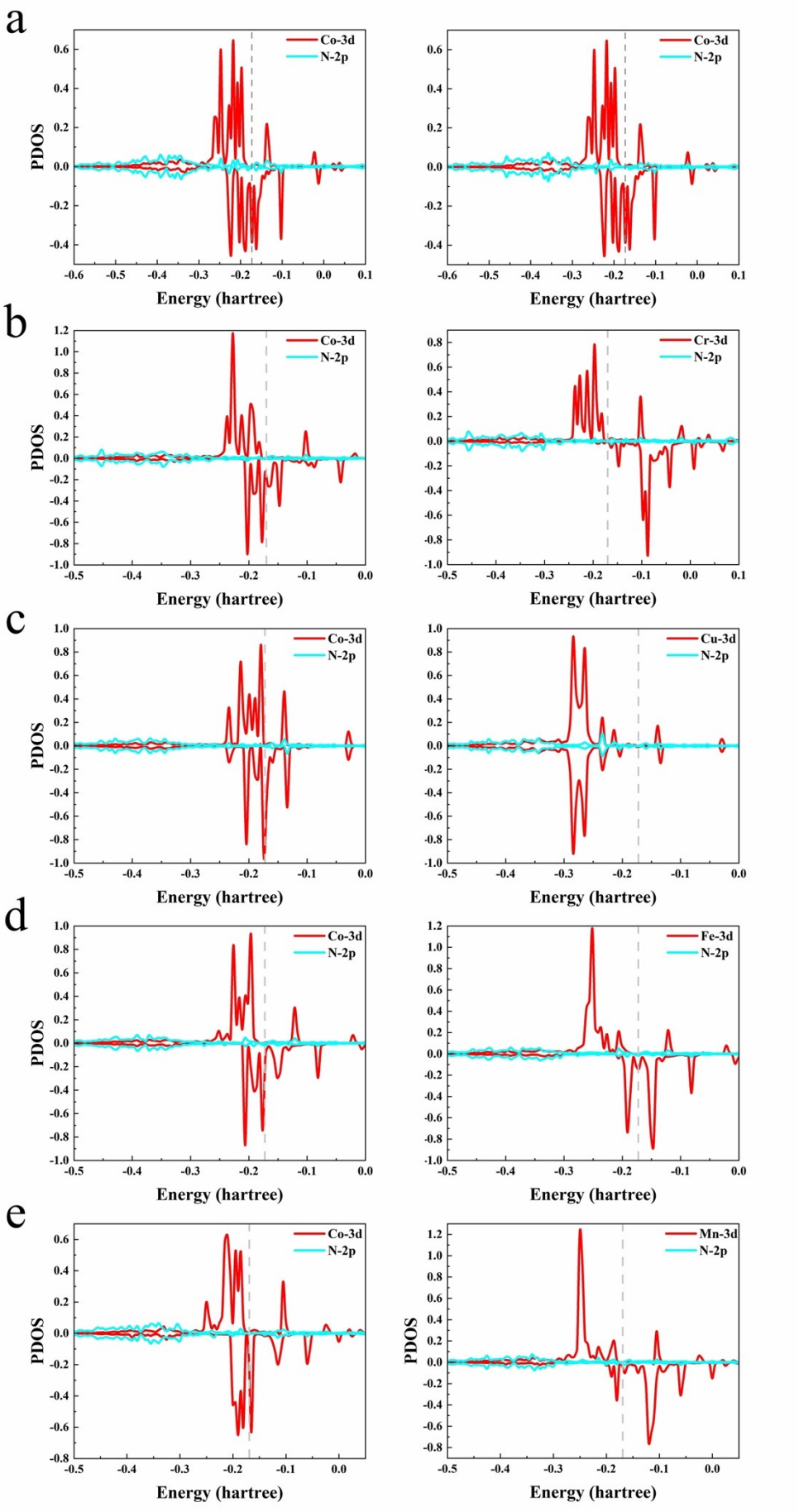
a
Co-3d
N-2p
PDOS
Energy (hartree)
b
Co-3d
Cr-3d
N-2p
c
Co-3d
Cu-3d
d
Co-3d
Fe-3d
e
Co-3d
Mn-3d

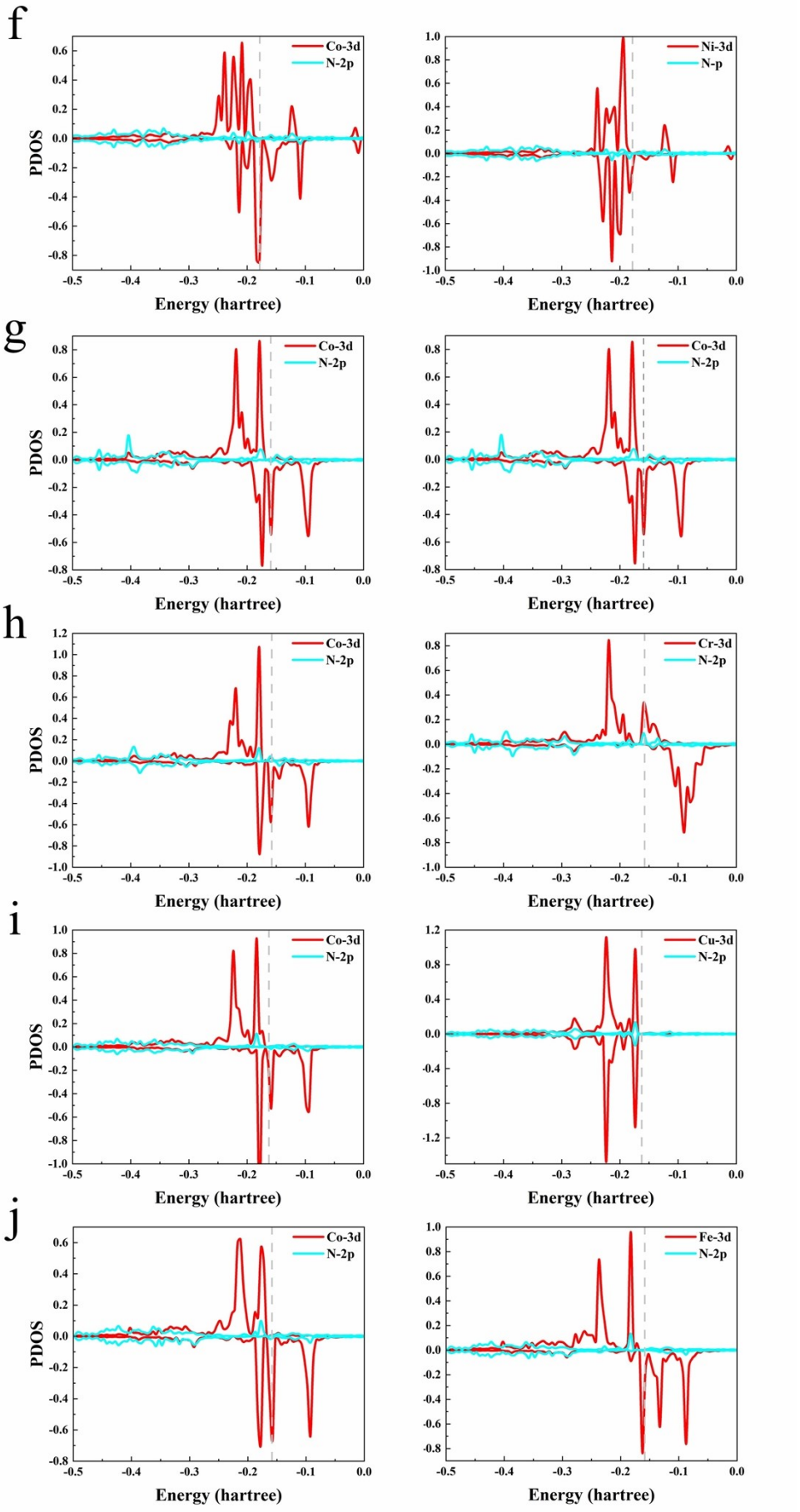
f
Co-3d
N-2p
Ni-3d
N-p
PDOS
Energy (hartree)
g
Co-3d
N-2p
Co-3d
N-2p
PDOS
Energy (hartree)
h
Co-3d
N-2p
Cr-3d
N-2p
PDOS
Energy (hartree)
i
Co-3d
N-2p
Cu-3d
N-2p
PDOS
Energy (hartree)
j
Co-3d
N-2p
Fe-3d
N-2p
PDOS
Energy (hartree)

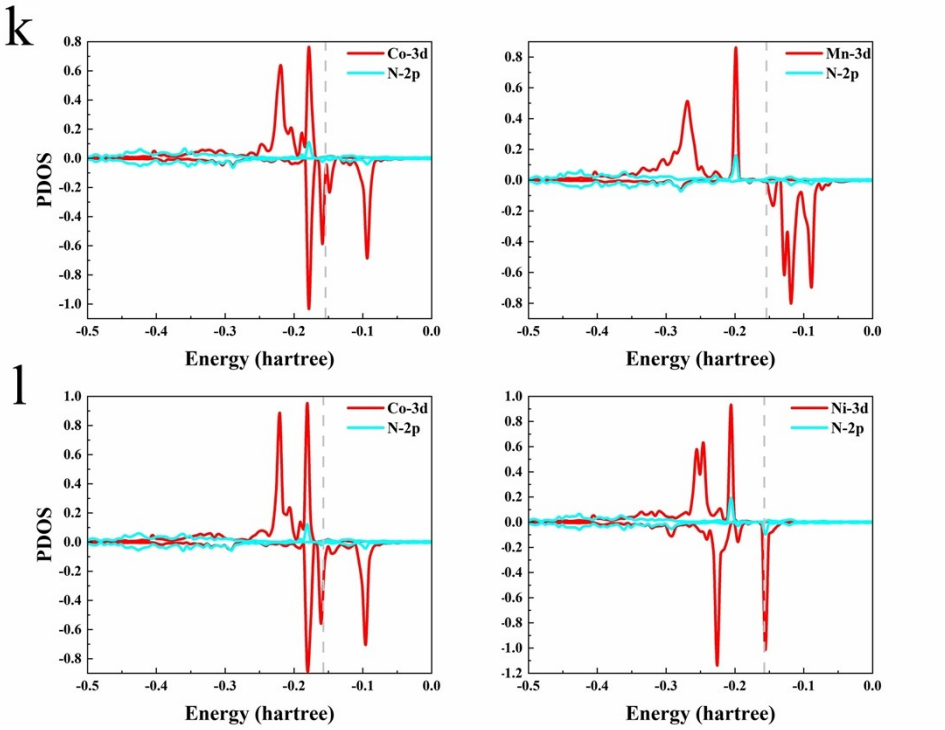

Fig. S2 a-f are the Partial Density of States (PDOS) of metal atoms and nitrogen atoms in M^1N_3-M^2N_3@NGr-a, and g-l are the PDOS of metal atoms and nitrogen atoms in M^1N_3-M^2N_3@NGr-s (with M^1=Co and M^2=Co, Cr, Cu, Fe, Mn, Ni).

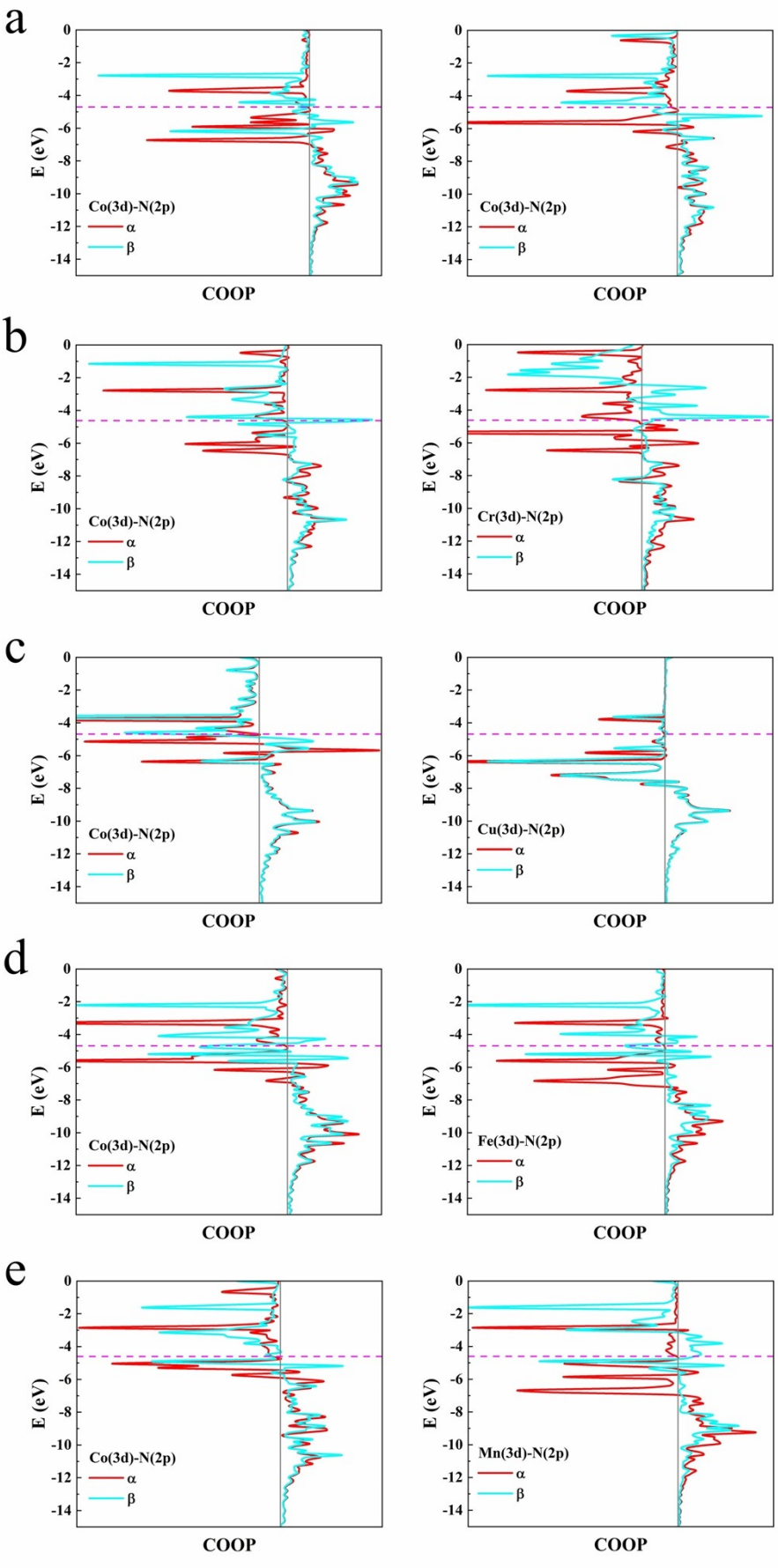
a
b
c
d
e
E (eV)
0
-2
-4
-6
-8
-10
-12
-14
Co(3d)-N(2p)
α
β
COOP
Co(3d)-N(2p)
α
β
COOP
Co(3d)-N(2p)
α
β
COOP
Cr(3d)-N(2p)
α
β
COOP
Co(3d)-N(2p)
α
β
COOP
Cu(3d)-N(2p)
α
β
COOP
Co(3d)-N(2p)
α
β
COOP
Fe(3d)-N(2p)
α
β
COOP
Co(3d)-N(2p)
α
β
COOP
Mn(3d)-N(2p)
α
β
COOP

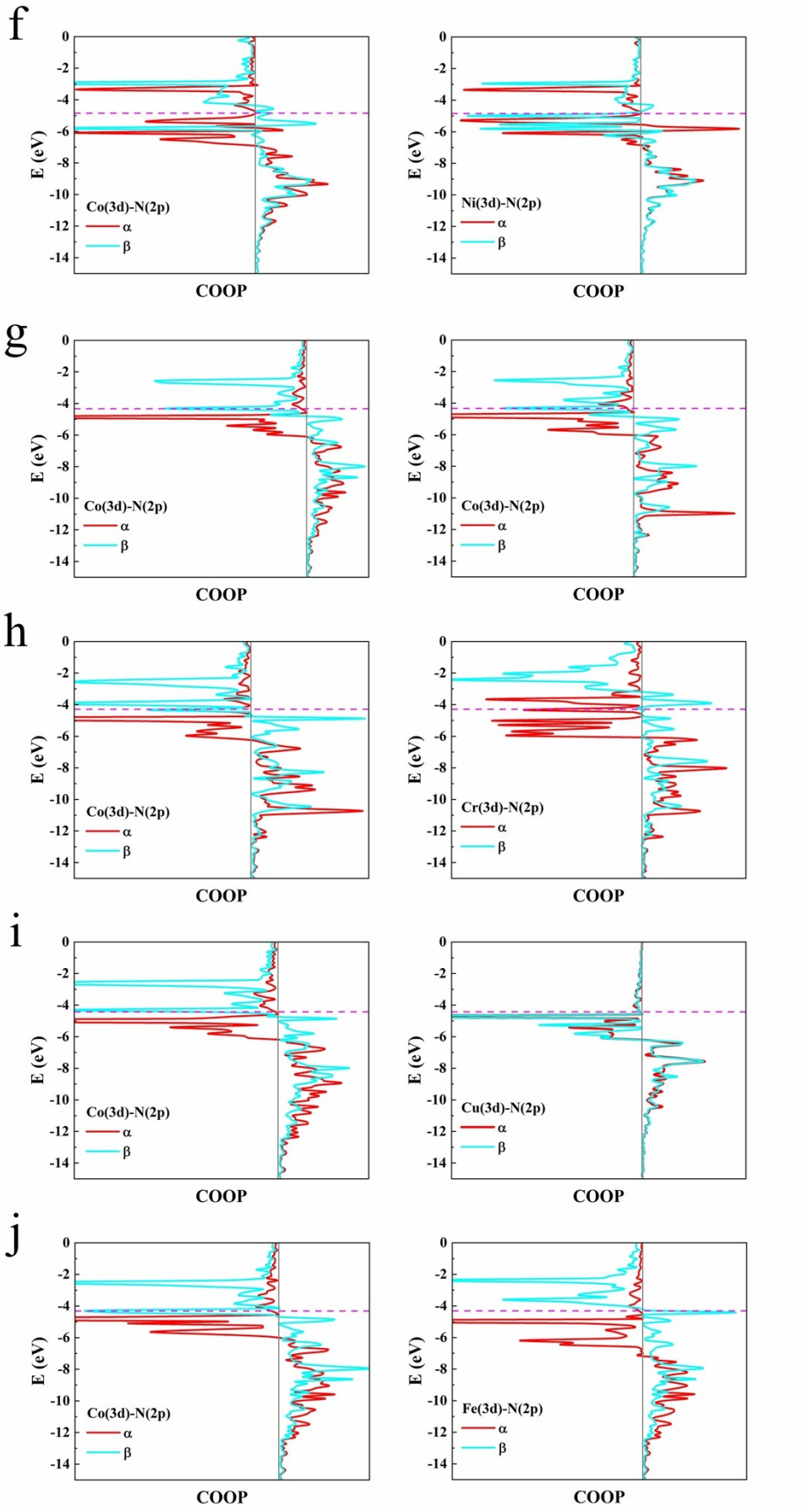
f
g
h
i
j
E (eV)
COOP
Co(3d)-N(2p)
Ni(3d)-N(2p)
Cr(3d)-N(2p)
Cu(3d)-N(2p)
Fe(3d)-N(2p)
α
β
0
-2
-4
-6
-8
-10
-12
-14

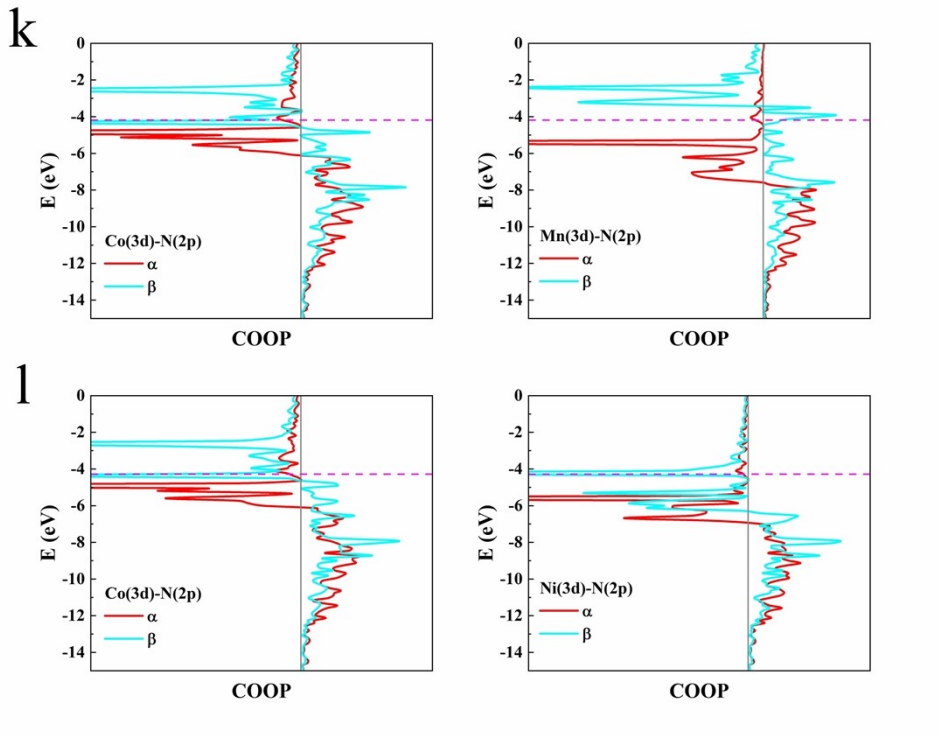

Fig. S3 a-f are the Crystal Orbital Overlap Population (COOP) of metal atoms and nitrogen atoms in M^1N_3-M^2N_3@NGr-a, and g-l are the COOP of metal atoms and nitrogen atoms in M^1N_3-M^2N_3@NGr-s (with M^1=Co and M^2=Co, Cr, Cu, Fe, Mn, Ni).

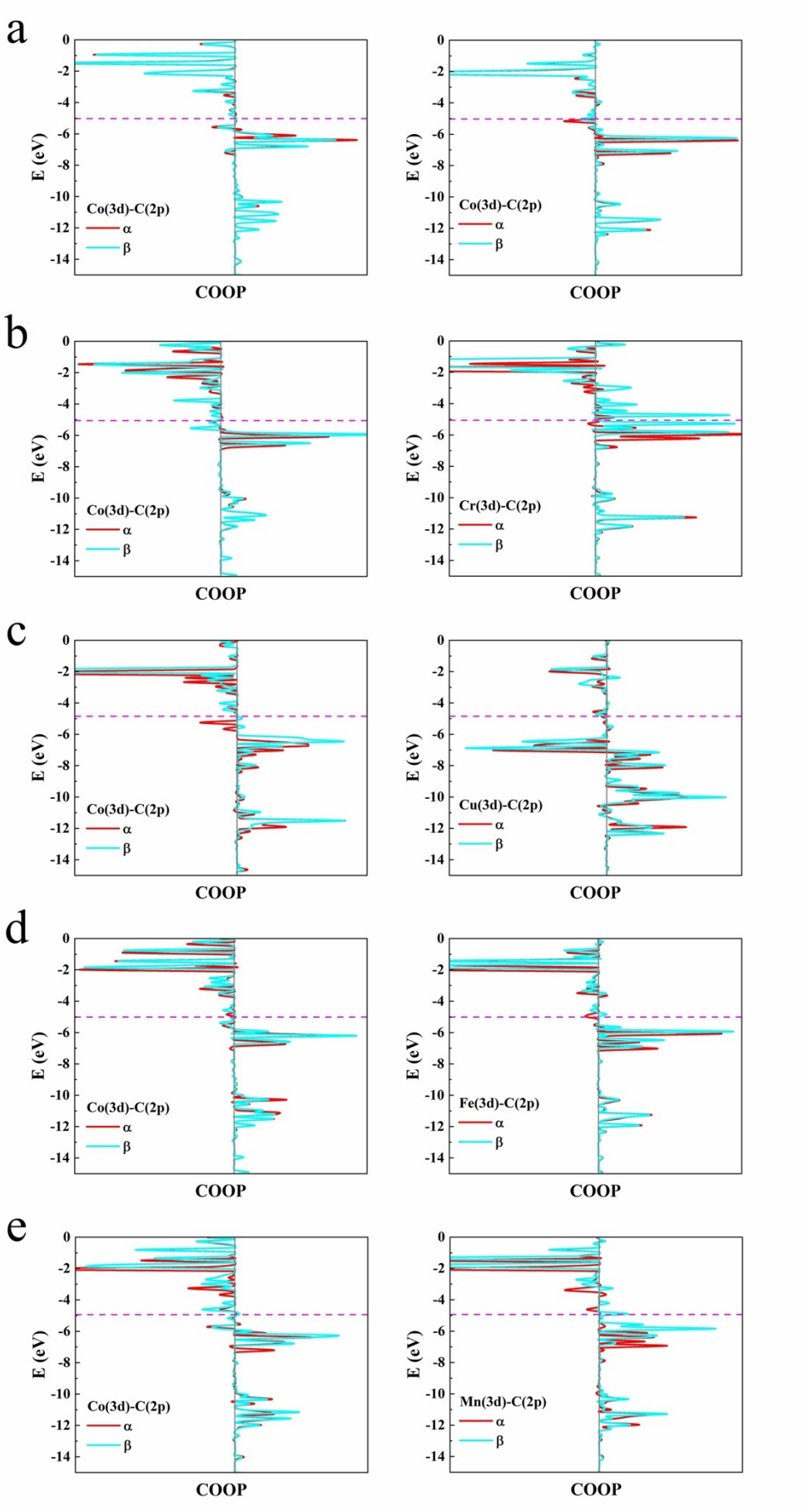
a
b
c
d
e
E (eV)
COOP
Co(3d)-C(2p)
Cr(3d)-C(2p)
Cu(3d)-C(2p)
Fe(3d)-C(2p)
Mn(3d)-C(2p)
α
β
0
-2
-4
-6
-8
-10
-12
-14

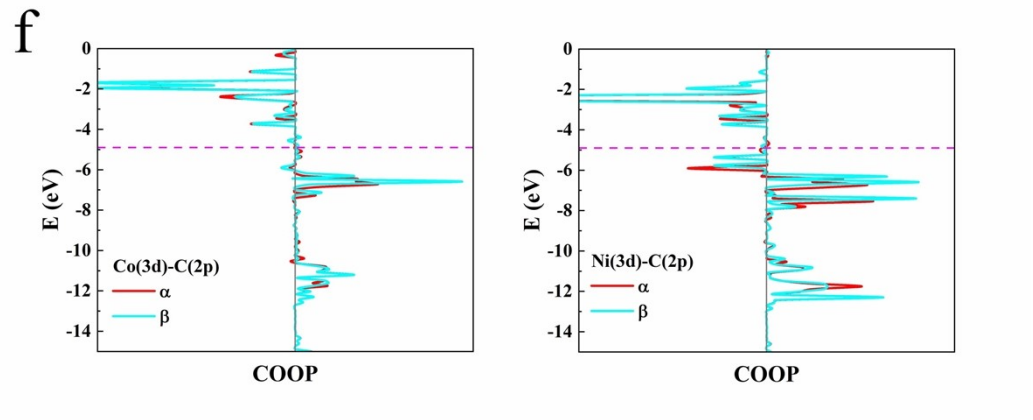

Fig. S4 a-f are the COOP of metal atoms and carbon atoms in the intermediate (*CO*CO) of M^1N_3-M^2N_3@NGr-a (with M^1=Co and M^2=Co, Cr, Cu, Fe, Mn, Ni).

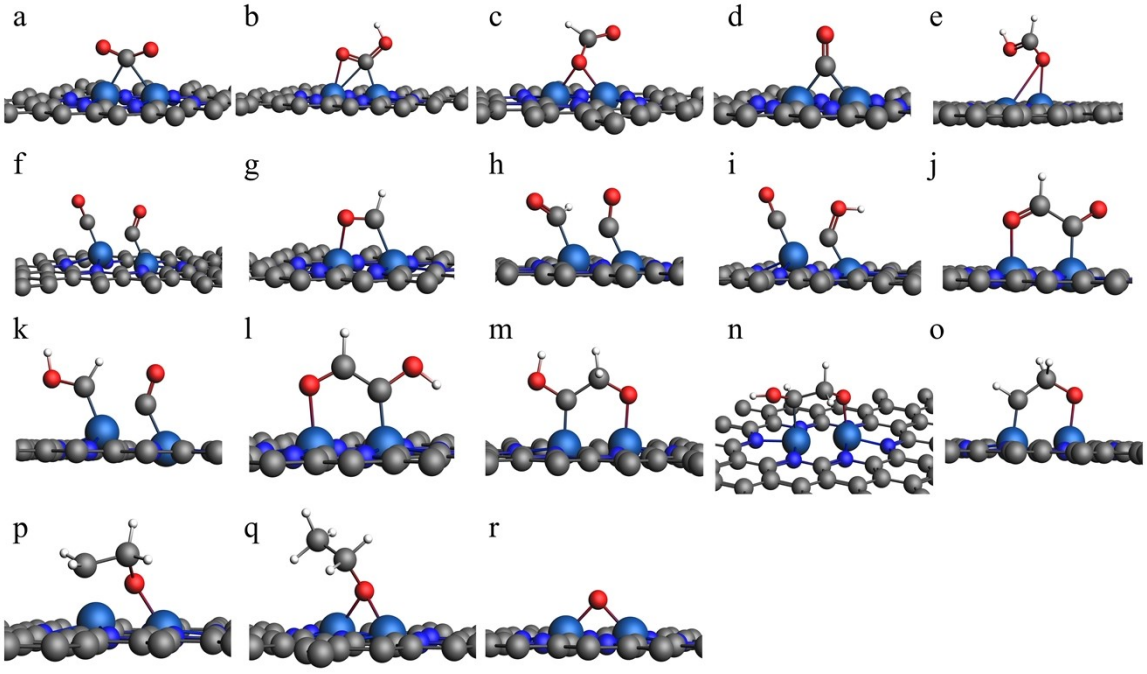

Fig. S5 The structural optimization model for key reaction intermediates of CoN_3-CoN_3@NGr-a.

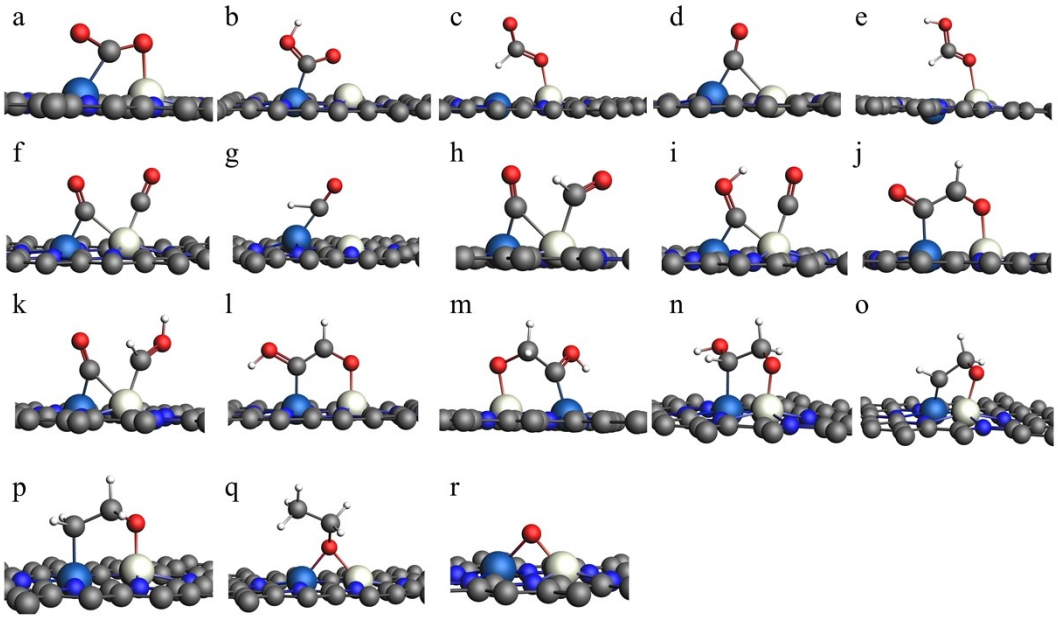

Fig. S6 The structural optimization model for key reaction intermediates of CoN_3-CrN_3@NGr-a.

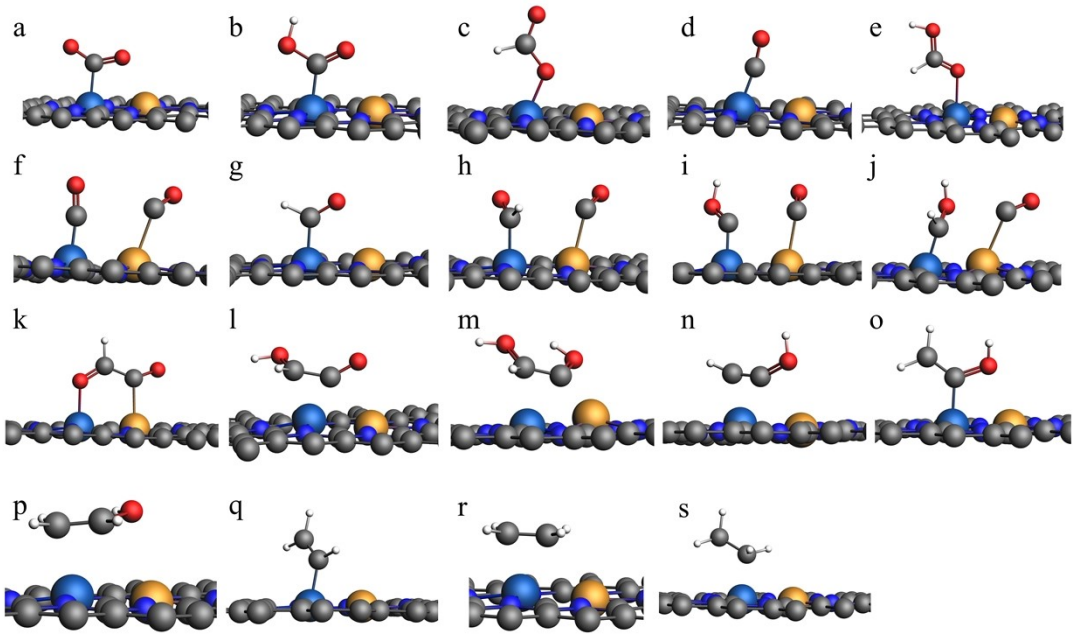

Fig. S7 The structural optimization model for key reaction intermediates of CoN_3-CuN_3@NGr-a.

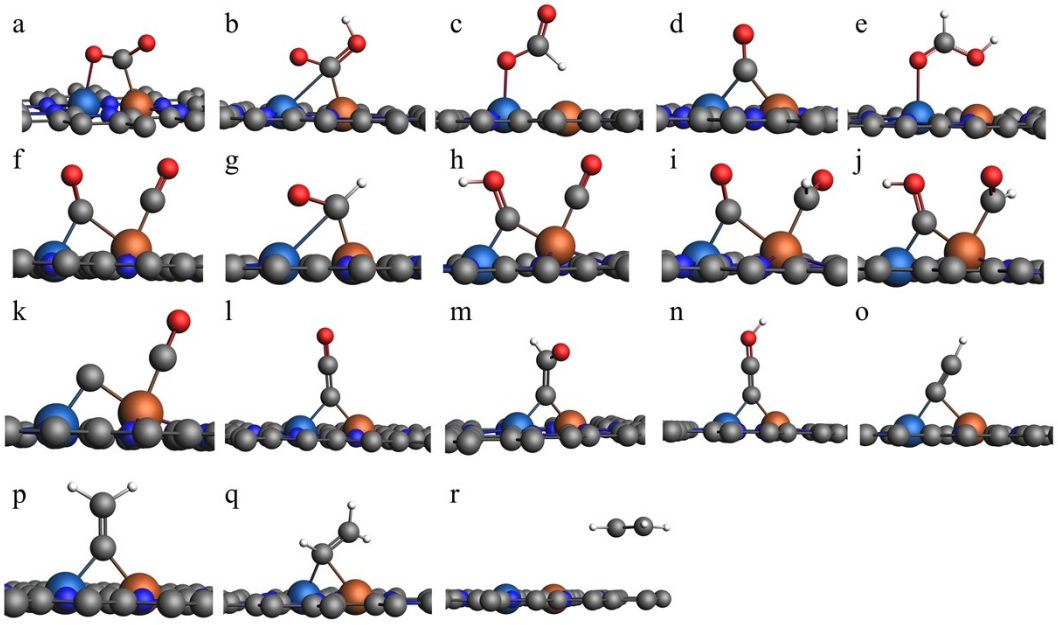

Fig. S8 The structural optimization model for key reaction intermediates of CoN_3-FeN_3@NGr-a.

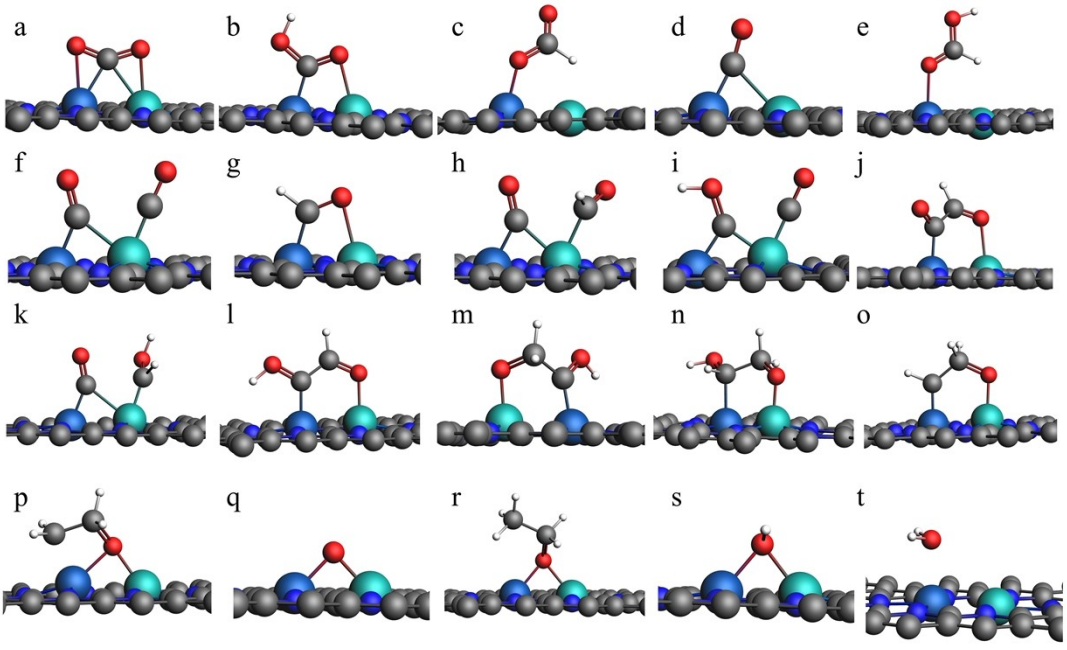

Fig. S9 The structural optimization model for key reaction intermediates of CoN_3-MnN_3@NGr-a.

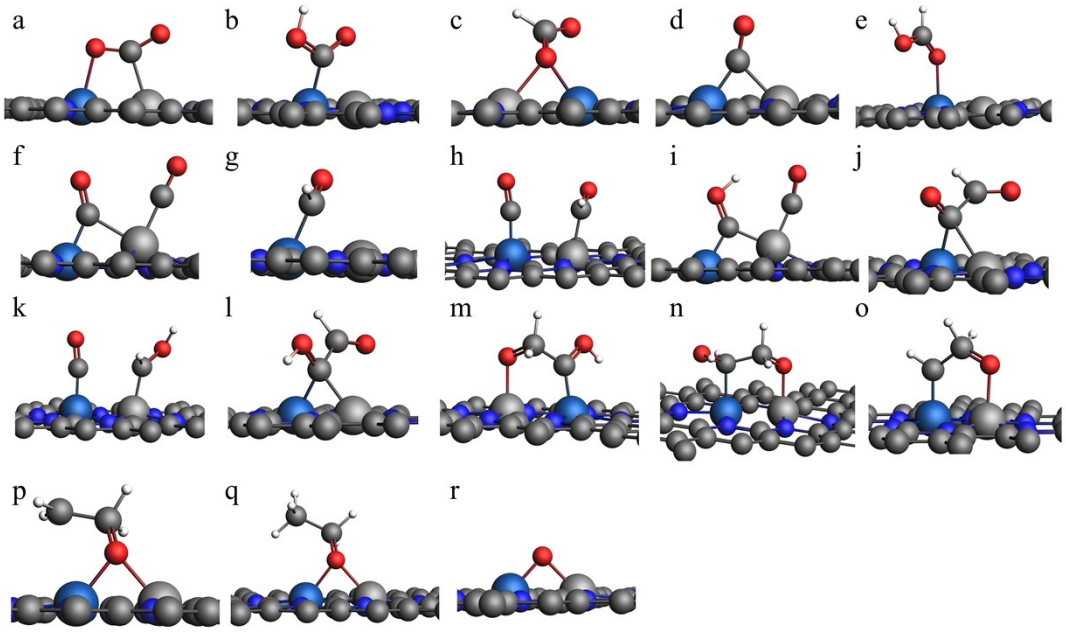

Fig. S10 The structural optimization model for key reaction intermediates of CoN_3-NiN_3@NGr-a.